Neuroscience Research 71 (2011) 49–62

Contents lists available at ScienceDirect

Neuroscience Research

journal homepage: www.elsevier.com/locate/neures

Phasic reward responses in the monkey striatum as detected by voltammetry with diamond microelectrodes

Kenji Yoshimi[a,b,*], Yuuki Naya[c], Naoko Mitani[c], Taisuke Kato[c], Masato Inoue[a], Shihoko Natori[a,d], Toshimitu Takahashi[a], Adam Weitemier[e], Natsuko Nishikawa[a,d], Thomas McHugh[e], Yasuaki Einaga[c], Shigeru Kitazawa[a,b]

[a] Department of Neurophysiology, Juntendo University School of Medicine, Hongo 2-1-1, Bunkyo-ku, Tokyo 113-8421, Japan
[b] CREST, Japan Science and Technology Agency, Honcho 4-1-8, Kawaguchi-shi, 15 Saitama 305-8575, Japan
[c] Department of Chemistry, Keio University, 3-14-1 Hiyoshi, Yokohama 223-8522, Japan
[d] Department of Neurology, Juntendo University School of Medicine, Hongo 2-1-1, Bunkyo-ku 113-8421, Japan
[e] RIKEN BSI, Wako, Saitama, Japan

ARTICLE INFO

Article history:
Received 27 June 2010
Received in revised form 16 April 2011
Accepted 18 May 2011
Available online 27 May 2011

Keywords:
Reward
Dopamine
Boron-doped diamond
Amperometry
Voltammetry
Striatum
Caudate
Primate

ABSTRACT

Reward-induced burst firing of dopaminergic neurons has mainly been studied in the primate midbrain. Voltammetry allows high-speed detection of dopamine release in the projection area. Although voltammetry has revealed presynaptic modulation of dopamine release in the striatum, to date, reward-induced release in awakened brains has been recorded only in rodents. To make such recordings, it is possible to use conventional carbon fibres in monkey brains but the use of these fibres is limited by their physical fragility. In this study, constant-potential amperometry was applied to novel diamond microelectrodes for high-speed detection of dopamine. In primate brains during Pavlovian cue-reward trials, a sharp response to a reward cue was detected in the caudate of Japanese monkeys. Overall, this method allows measurements of monoamine release in specific target areas of large brains, the findings from which will expand the knowledge of reward responses obtained by unit recordings.

1. Introduction

Midbrain dopaminergic neurons are thought to transmit reward and reward-prediction signals to forebrain areas. Transient, sharply time-locked burst responses have been observed repeatedly in unit recordings of midbrain dopamine neurons (Fiorillo et al., 2003; Matsumoto and Hikosaka, 2009; Joshua et al., 2008; Takikawa et al., 2004; Schultz et al., 1993, 1997; Schultz, 2007). However, whether the chemical transmission at dopaminergic terminals linearly reflects the number of impulses transmitted by midbrain dopamine neurons is not well understood. First, the release can be modulated by facilitation and depression, depending on the firing history (Abeliovich et al., 2000; Garris et al., 1999; Kita et al., 2007; Phillips et al., 2002; Yavich, 1996; Zhang et al., 2009). Second, several factors, e.g., psychostimulants and nicotine, modulate dopamine release at synaptic terminals (Schmitz et al., 2003).

Dopamine detection using fast-scan cyclic voltammetry (FSCV) on carbon fibres has been highly successful in the past decade because of their high sensitivity and fast temporal resolution (Hafizi et al., 1990; Heien et al., 2004; Marsden et al., 1988; Kawagoe et al., 1993; Bath et al., 2000). In this study, we sought to perform high-speed electrochemical detection of dopamine in the striatum of behaving monkeys. In an early investigation of direct electrochemical recording of dopamine in the primate brain (Lindsay et al., 1981), the sampling speed was of the order of minutes. Gerhardt et al. (1996) recorded dopamine release in the monkey striatum using chronoamperometry with a carbon fibre; however, the monkey was anaesthetized. Cragg et al. (2002) recorded phasic dopamine release in the striatum of marmosets, but in this study brain slices were used. Shon et al. (2010) recorded evoked dopamine release in the striatum of the pig whose brain is as large as those of the monkeys; however, the animal was also anaesthetized.

Abbreviations: AA, ascorbate; DA, dopamine; FSCV, fast-scan cyclic voltammetry; BDD, boron-doped diamond; MFB, medial forebrain bundle; MRI, magnetic resonance imaging; PBS, phosphate-buffered saline; DOPAC, 3,4-dihydroxyphenylacetic acid; SW, square-wave differential pulse-voltammetry.

* Corresponding author at: Department of Neurophysiology, Juntendo University School of Medicine Hongo 2-1-1, Bunkyo-ku, Tokyo 113-8421, Japan.
Tel.: +81 3 3813 3111; fax: +81 3 3813 4954.
E-mail address: yoshimik@juntendo.ac.jp (K. Yoshimi).

0168-0102/$ – see front matter © 2011 Elsevier Ireland Ltd and the Japan Neuroscience Society. All rights reserved.
doi:10.1016/j.neures.2011.05.013

The carbon fibres used widely in rodents are easy to snap; special caution is required for their insertion into the brain (Phillips and Wightman, 2003). For implantation in large brains, such as those of monkeys, it is clear that the implantation of carbon fibre microelectrodes would be restricted not only by the dura mater, but also by fissures and the choroid plexus. Because tungsten needles are widely used for electrophysiological recording in deep parts of primate brains, tungsten can be used to make an electrochemical probe for monkey brains. Because the surface of tungsten is not suitable for electrochemical detection of dopamine, in this study, a tungsten needle (0.3-mm diameter) was covered with boron-doped diamond (BDD) for use as an electrochemical probe. In general, diamond electrodes have wide voltage windows, low background current and low adsorption (Einaga et al., 2004; Fujishima et al., 2005). Recently, growing evidence has suggested the potential use of BDD as an electrochemical sensor. Furthermore, we have already shown that a diamond microelectrode on thin tungsten wire can be used for *in vivo* dopamine detection in the anaesthetized mouse brain (Suzuki et al., 2007). Whereas pulse voltammetry was used in the former study, we noticed that our novel diamond microelectrode could detect low concentration of dopamine on constant-potential amperometry. Using this technology, we observed a sharp increase in electrochemical current in the monkey striatum following a reward-predicting cue.

2. Materials and methods

2.1. Animals

Two Japanese monkeys (*Macaca fuscata*, male, 10 and 6 kg) participated in the reward experiments. One further monkey (male, 10 kg) and three C57BL/6J mice (male, 4–6 months old, Charles River Laboratories, Yokohama, Japan) were used for *in vivo* measurement of dopamine release evoked by electrical stimulation. The procedures were in accordance with the Guidelines for Proper Conduct of Animal Experiments established by the Science Council of Japan, and all experiments were approved by the Ethics Review Committee for Animal Experimentation of Juntendo University School of Medicine. All possible efforts were made to minimize the number of animals used and their suffering.

2.2. Electrochemical probes

2.2.1. Diamond microelectrodes

Boron-doped diamond (BDD) was formed on the surface of tungsten needles (0.3 mm diameter, 30 mm long) as previously described (Suzuki et al., 2007), except that the thin tungsten filaments were replaced by needles, and the boron doping in the carbon source was increased to 5%, from 1% in the previous study. In short, a thin diamond layer was formed on sharp tungsten needles by placing the needles in plasma with vapour from acetone and trimethoxyborane. The shaft of the microelectrode was connected to a stainless tube, yielding a microelectrode of 150 mm in length. The elongated shaft was insulated with cashew resin (Cashew Co. Ltd., Tokyo, Japan), excluding 1 mm from the tip (Fig. 1A). The surface of the diamond was oxidized with +2.5 V in 0.1 N HCl. Oxidization of the diamond surface improved dopamine selectivity at relatively low potentials (Suzuki et al., 2007).

2.2.2. Carbon fibre microelectrodes

Carbon fibre microelectrodes (Fig. 1A) were prepared as previously described (Natori et al., 2009; Oyama et al., 2010). Individual carbon fibres (7 μm in diameter, HTA-7, Toyo-RENAX, Tokyo, Japan) were sealed in pulled glass capillary tubes with epoxy-resin, such that 300 μm of the carbon fibres protruded from the capillary tubes.

2.3. Chemicals

Chemical reagents, including dopamine HCl (DA), serotonin HCl (5-HT), noradrenaline (NA), 3,4d-dihydroxyphenylacetic acid (DOPAC), ascorbate and nomifensine maleate, were purchased from Sigma-Aldrich (St. Louis, MO, USA). The other special-grade reagents were purchased from WAKO (Tokyo, Japan). To stabilize the pH of the solution, our phosphate-buffered saline (PBS) was 0.9% NaCl buffered with 100 mM phosphate-buffer (pH 7.4). To prepare acidic (pH 7.2) and basic (pH 7.6) pH-shifted buffers, 72.8 μl of 1 N HCl or 60.4 μl of NaOH, respectively, were added to 10 ml of PBS.

2.4. Electrochemistry

Constant potential amperometry was performed with the diamond microelectrode using a commercial control/recording system

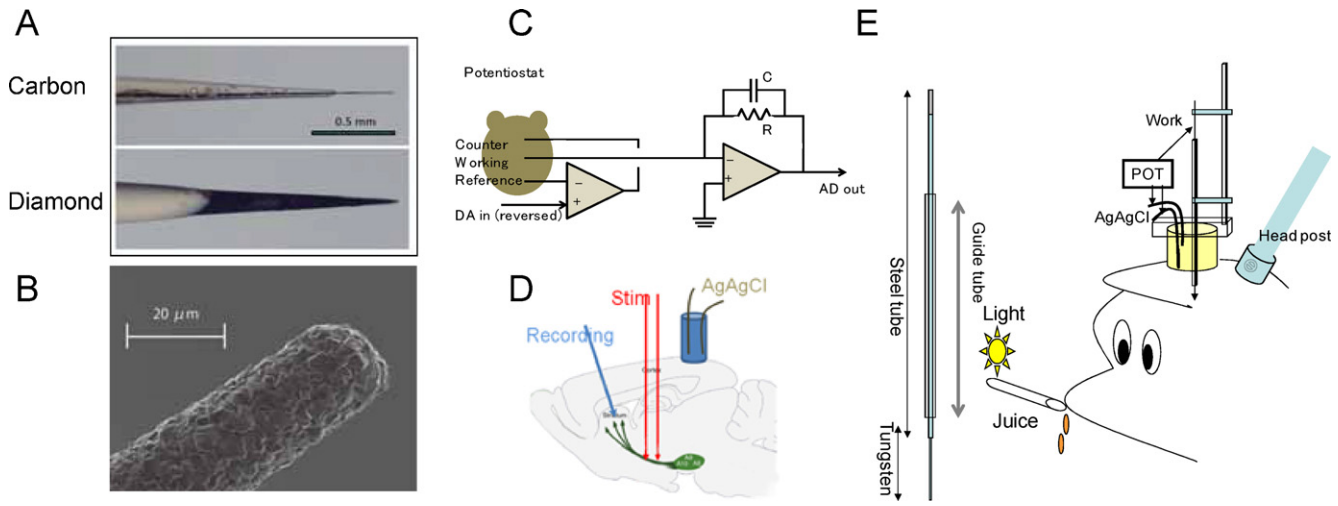

Fig. 1. Experimental methods. (A) Side view of the tips of carbon fibre (Cf) and diamond microelectrode (BDD). Scale bar = 500 μm. (B) Scanning electron microgram of the tip of the diamond microelectrode. (C) Circuit of potentiostat. (D) Electrode positions for the recordings in mouse brains. (E) Left: elongated diamond microelectrode and guide cannula. Right: microelectrode positions on the monkey head. POT: potentiostat.

(TH-1; ESA Biosciences Inc., MA, USA). Electrodes were connected to our custom-made potentiostat (Fig. 1C) or a commercial potentiostat (HECS-974D, Huso Electrochemical Systems, Kawasaki, Japan). The working, reference and counter electrodes were connected to the potentiostat. The gain of the amplifier was 1000 nA/V for carbon fibre FSCV, 10,000 nA/V for diamond FSCV, 50 nA/V for square-wave differential pulse voltammetry (SW) and 20 nA/V for constant-potential amperometry. The time constant was 0.2 ms for FSCV and SW, but 20 ms for constant-potential amperometry. Potential delivery and data sampling were controlled by the TH-1 system. During amperometry, the diamond microelectrode was held at +0.6 V against the Ag/AgCl reference electrode, and the average current for 20 ms was sampled at 10, 25 or 50 Hz. Data sampled at 25 or 50 Hz were down-sampled to 12.5 Hz by taking the average of adjacent data points.

Diamond microelectrodes were calibrated *in vitro* using a flow-cell with a small fountain (0.06-ml capacity) with two Ag/AgCl wires and flow of PBS constantly at 10 ml/min. The solution was switched to 40, 200, or 1000 nM dopamine in PBS during the electrochemical recordings for calibrations. For characterization of the microelectrodes, FSCV and SW (Bard and Faulkner, 2002; Oyama et al., 2010) were also tried *in vitro* (Fig. 2 top and middle). FSCV was performed with the carbon-fibre microelectrodes (−0.4 to 1.3 V, against Ag/AgCl, 400 V/s) as previously described (Kawagoe et al., 1993; Heien et al., 2004; Phillips and Wightman, 2003; Natori et al., 2009) and also on diamond microelectrodes (−0.2 to 1.5 V, against Ag/AgCl, 400 V/s). Differential pulse voltammetry using square-wave pulses consisted of 10 voltage-pulse stairs with a pair of high and low pulses (Fig. 2 middle-left), and the differential current between the adjacent steps at high and low pulses was calculated at the various potentials (Bard and Faulkner, 2002; Nakazato and Akiyama, 1999; Oyama et al., 2010; Suzuki et al., 2007). By excluding the first 6 ms of each 20 ms pulse, the influence of capacitative current was minimized.

2.5. In vivo validation by evoked dopamine release

Evoked dopamine release was evaluated in the striatum of anaesthetized mice as previously described (Natori et al., 2009; Oyama et al., 2010; Yavich, 1996; Yavich and Tiihonen, 2000). C57BL/6 mice were anaesthetized initially with pentobarbital (50 mg/kg, i.p.), held on a stereotaxic frame (Narishige, Tokyo, Japan) and maintained with 1% isoflurane inhalation. Carbon-fibre and diamond microelectrodes were bundled in parallel 0.5 mm apart and inserted into the striatum (electrode tip position at 0.5 mm anteriorly, 2 mm laterally and 3.0 mm ventrally relative to bregma with a 15° forward angle), according to the mouse brain atlas (Franklin and Paxinos, 1997). Two Ag/AgCl wires (reference and auxiliary electrodes) were combined in a glass tube filled with 3% agar made with PBS and placed on the dural surface. A pair of stainless steel bipolar stimulating electrodes (Unique Medical Co., Japan; distance between the poles: 1 mm; the stainless needle was insulated except for the 0.3-mm tip) was implanted in the medial forebrain bundle (MFB; P, −2.0 mm; L, 1.1 mm; V, −5.0 mm, Fig. 1D). The dorso-ventral placement of the stimulating electrode was adjusted to obtain the maximal dopamine response. Biphasic constant current pulses were delivered to the MFB (30 Hz; biphasic 200 μA constant current, 3–24 pulses, 2 ms each) through the stimulating electrodes with an isolated stimulator (SS-202J connected to SEN-7203, Nihon-Koden, Co., Tokyo. Japan). The pulse stimulated the nigrostriatal tract, and evoked dopamine release in the dorsal striatum was recorded with the diamond microelectrode and with the carbon fibre for comparison.

Similar MFB stimulation was attempted in a monkey. The monkey was anaesthetized with ketamine and medetomidine and held on a stereotaxic frame (Narishige, Tokyo, Japan). The glass-coated tungsten electrodes (FHC, Bowdin, ME, USA) were penetrated vertically, aiming at the right subthalamic nucleus (STN). The positions of the thalamic ventral–lateral nucleus (VL) and the STN on the electrode tracks were identified using a regular unit-recording amplifier (PLEXON, Dallas, TX, USA). Because a thick bundle of tyrosine-hydroxylase-positive axons was histologically observed at the medio-dorsal edge of the STN, the electrode was placed at the estimated position of the bundle, and electrical stimulation was delivered. The diamond microelectrode was placed in the striatum, and the electrochemical response to the stimulation was recorded.

2.6. In vivo recording in behaving monkeys

A chronic recording chamber and a head holder were implanted in the monkey skull while anaesthetized with pentobarbital sodium (Fig. 1E). The chamber was placed above the right striatum. Coronal and sagittal images of the head and brain were taken beforehand with a 0.3-T magnetic resonance scanner (AIRIS2, Hitachi Medical Co., Tokyo, Japan) to determine the position of implantation for each monkey (Figs. 6 and 7). The relative position of the chamber from the caudate (18–22 mm anterior, 4–8 mm lateral from the interaural centre, and 14–18 mm ventral from the brain surface) was estimated from the MRI images. Unit recordings were also used to verify the relative depth of the caudate from the chamber.

The diamond microelectrode was set on a manipulator (MO-95, Narishige, Tokyo, Japan) and inserted into the caudate through a stainless steel guide-tube that was placed 10–15 mm above the recording target. Two Ag/AgCl wires were placed above the dura mater and used as reference and counter electrodes. After the *in vivo* recordings, the used diamond microelectrode tips were immediately rinsed, kept in saline, and calibrated with dopamine solutions. The sensitivity deteriorated often (Table 3) but was recovered after cleaning in a sonication bath filled with heated detergent solution and a brief dip in isopropanol and 0.1 N HCl.

The animals were seated in a primate chair and well-habituated to the task in advance, with their heads held with the head holder (Fig. 1E). A tube was placed in front of the mouth for juice delivery (0.5 ml/0.25 s), and a light-emitting diode (LED) was placed 10 cm from the eyes to deliver conditioning light stimuli (CS). During the recordings, their behaviour was observed. Trials were excluded from further analysis when the animal did not stay calm. Juice was delivered at intervals of 10–20 s. In the other reward schedule, a light flash by a brief illumination of LED served as a conditioned stimulus in a Pavlovian conditioning paradigm. A light stimulus of 0.2-s duration preceded juice delivery by 1.0 (monkey K) or 2.0 s (monkey S). To verify the effect of the conditioned stimulus, the light was shielded with cardboard in some trials, whereas the light was visible in others (shielded and visible trials, respectively). Juice delivery was occasionally omitted after the light stimulus. Thus, there were three types of trials: one with the light stimulus and the juice reward ("paired" trials, P), another with light without juice ("light" trials, L), and the third type with juice without the preceding light stimulus ("juice" trials, J).

Monkeys received 100–200 juice deliveries per day for 5 days per week, and amperometric recording was performed once or twice a week. Water was restricted to 200 ml/day on weekdays and available *ad libitum* in the home cage from Friday evening to Sunday morning.

2.7. Data analysis

For verification of the detection sensitivity *in vitro*, the signal to noise ratio (S/N) and the detection limit were calculated. S/N was determined by dividing the response amplitude (8 s after switch-

ing to the test solution) by the standard deviation (SD) during the baseline period before switching. The detection limit was estimated as the minimal concentration of dopamine that evoked a response three times as large as the standard deviation of the measurements during the baseline period.

Constant-potential amperometry (Fig. 2 bottom) requires larger amplification and is susceptible to noise artefacts created by animal movements. It was potentially useful, however, for a monkey whose head movement was restricted by a steel restrainer (head-post). For the analysis of amperometric current during monkey behavioural tasks, noisy data were excluded based on the following 3-step rule. (1) The trial was excluded if the animal did not stay calm. The extra movements during the recordings were frequent in the early sessions but became less frequent as the animals habituated to the task (Table 3). Many of the recorded trials associated with superfluous movement of the monkey had large noises, more than 1000 pA. (2) Therefore, if the deviation between the maximal and minimal current value during the recording period exceeded 1000 pA, the trial was excluded. (3) Among the remaining trials, the mean and SD of the deviation were calculated, and then trials with deviations of more than mean + 2 SD were excluded from further analysis. The numbers of excluded trials are presented in Table 3. The response was measured from the baseline, which was defined as the mean signal during a 1-s period before the onset of each event.

The time-course for 3 s after the cue onset was analysed first by one-way analysis of variance (one-way ANOVA) over 41 time points, 4 before and 37 after the light onset. After significant

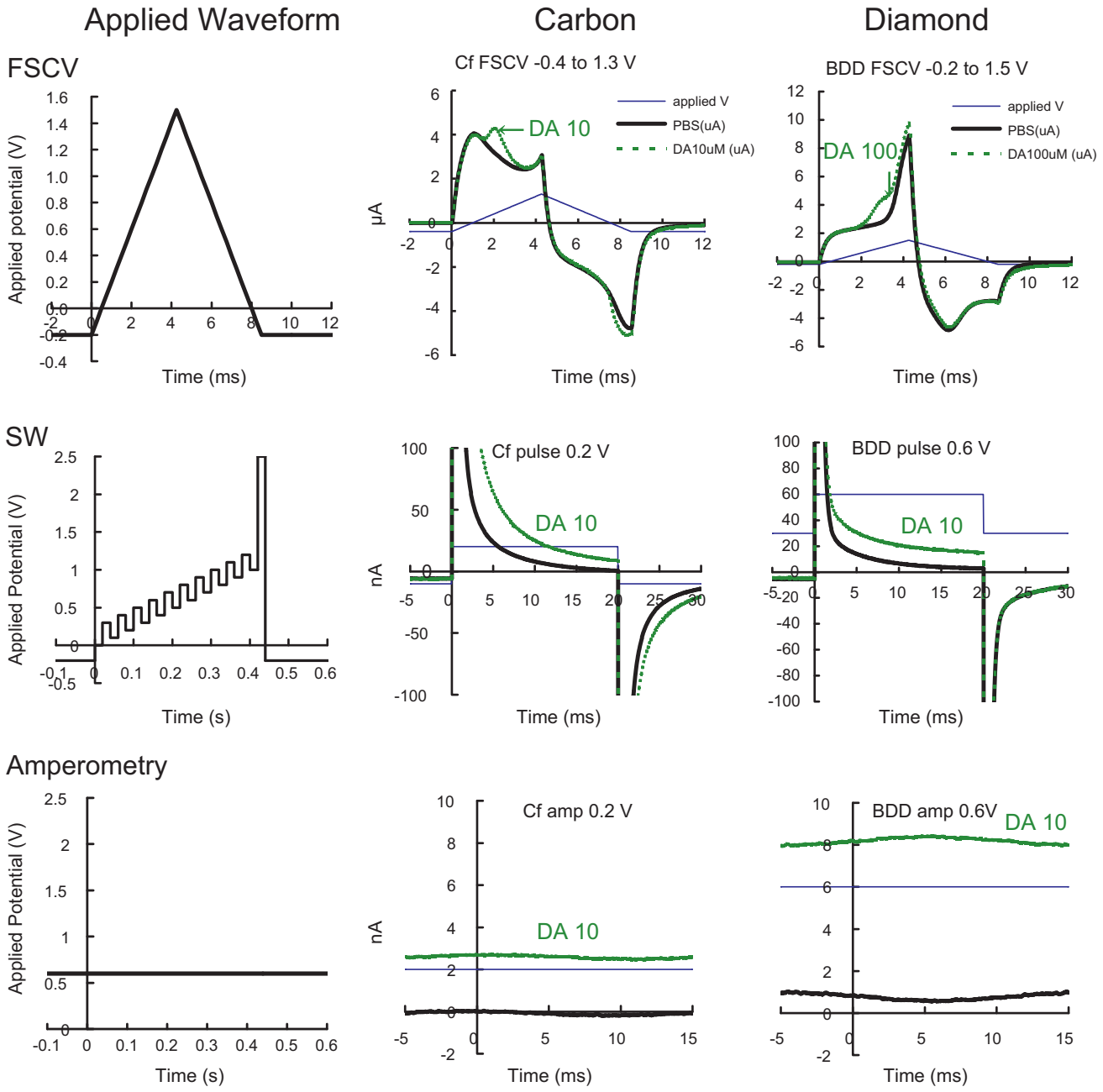

Fig. 2. Applied waveforms and current recordings for fast-scan cyclic voltammetry (FSCV, top), square-wave differential pulse voltammetry (SW, second bottom) and constant-potential amperometry (bottom). (Left) Applied potential against Ag/AgCl reference electrode. (Middle) Actual measured current for each waveform at carbon fibre. For square-wave, only one pulse is indicated. (Right) Measured current at diamond microelectrode. Typical recorded currents in PBS (black) and high (10 and 100 nM) concentrations of dopamine (green). (For interpretation of the references to colour in this figure legend, the reader is referred to the web version of the article.)

changes throughout the time-course were confirmed by ANOVA, the time points showing significant current increase were identified. When a post-event current was significantly larger ($p < 0.05$, Tukey's HSD test) than the largest point of the four pre-event values, it was regarded as a significant increase from baseline.

After evaluation of the time-course, two-way ANOVA was used to evaluate the two main effects of time (20 time points) and trial conditions (Paired, Light and Juice trials) and their interaction. SPSS (v17.0, IBM) software was used for the statistical analysis.

3. Results

3.1. Dopamine detection in vitro

Detection of dopamine and other electrochemically active chemicals was evaluated *in vitro*, at both carbon fibres and diamond microelectrodes (Figs. 2–4). Microelectrodes were placed in the flow of PBS, and the flow was switched to test solutions of 1 μM dopamine (DA), acidic pH 7.2 PBS (−pH), basic pH 7.6 PBS (+pH), 10 μM ascorbate (AA), 10 μM DOPAC and 1 μM serotonin (5-HT) solutions in PBS. Test solutions were sequentially applied for 10 s with 20-s intervals (Fig. 3). Three kinds of voltage application (FSCV, SW, and constant-potential amperometry) were tested (Figs. 2 and 3).

First, FSCV on a carbon fibre (−0.4 to +1.3 V, 400 V/s) yielded an intense current response to dopamine. With the triangular waveform, the dopamine oxidation current on carbon fibres had a peak of 2.6 ms from the onset of the voltage slope, which appeared to be at 600 mV (Fig. 2 top). At 2.6 ms after the onset of the slope, current responses were also induced by pH changes, DOPAC and 5-HT, but the response to ascorbate was low (Fig. 3 upper-left). Similar FSCV was also attempted using the diamond microelectrodes (−0.2 to +1.5 V, 400 V/s), but the response to dopamine was relatively weak (Fig. 3 upper-right). The current intensity at the peak potential of dopamine and the detection limit are summarized in Table 1. On the other hand, the response to pH and 5-HT was intense. The background-subtracted cyclic voltammograms of the test solutions are presented in Fig. 4 and supplemental figure Suppl. 1.

Second, SW was tested (Bard and Faulkner, 2002; Suzuki et al., 2007; Oyama et al., 2010). The responses at 200 mV (subtraction of the current at 200 mV and 0 mV pulse) and 600 mV are presented for a carbon fibre and 600 and 1000 mV for a diamond microelectrode (Fig. 3, second-bottom). With FSCV, the influence of capacitive current and the time for electron-transfer can affect the current (Fig. 2, middle). The result of SW is given as a simple function of the applied potential (Fig. 4).

The voltage-dependency of the diamond microelectrode was evaluated by SW. In the case of diamond microelectrodes, the oxidation of dopamine started at a lower voltage than that of pH, ascorbate and DOPAC (Fig. 4). Therefore, the 600 mV holding potential minimized the influence of these factors. However, the peak potential of 5-HT and NA was close to that of dopamine. The peak potential of dopamine was approximately 600 mV in most of the oxidized diamond microelectrodes. The peak voltage of dopamine varied slightly, presumably due to a surface oxidation condition, but only microelectrodes showing peak reactions to dopamine at 500–700 mV were chosen in the later studies. The result of SW is useful to evaluate voltage dependency of the electrochemical responses and determine the applied potential for amperometry.

Finally, constant-potential amperometry was tested. The current intensity was low in amperometry, but a nM level detection limit was achieved with the help of low noise (Table 1). During amperometry, the diamond microelectrode also responded to ascorbate, DOPAC and 5-HT. However, the influence of pH was negligible at both carbon fibre and diamond microelectrodes (Fig. 3 bottom).

Dopamine and 5-HT levels were temporally skewed in FSCV and SW (Fig. 3). The responses to test solutions of pH, ascorbate and DOPAC formed a plateau, whereas the current continued to increase in response to dopamine and 5-HT solutions, even after the solution in the test chamber was replaced. The solution in the chamber was estimated to be 90% replaced within 2 s. The adsorption was evaluated by remaining amplitude 10 s after PBS washout (Table 2). Although adsorption was negligible upon amperometry of DOPAC on diamond microelectrodes, adsorption was evident in FSCV on carbon fibres.

Table 1
Electrochemical dopamine detection *in vitro*.

		Current amplitude (nA)		Detection limit (nM)	
FSCV	Carbon	127.90	(±11.95)	3.1	(±0.4)
	Diamond	31.82	(±12.81)	147.0	(±69.6)
Amperometry	Carbon	0.24	(±0.04)	11.0	(±3.3)
	Diamond	1.12	(±0.17)	4.8	(±1.0)

Values are mean ± s.e.m. of 6 electrodes.

Table 2
Adsorption index.

		Dopamine		DOPAC	
FSCV	Carbon	0.24	(±0.02)	0.16	(±0.01)
	Diamond	0.07	(±0.10)	0.03	(±0.05)
Amperometry	Carbon	0.03	(±0.01)	0.01	(±0.00)
	Diamond	0.04	(±0.02)	0.03	(±0.01)

Values are mean ± s.e.m. of 6 electrodes. The index of adsorption at carbon fibres and diamond microelectrodes during flow-cell measurements. Adsorption index is the ratio of the remaining amplitude at 10 s after the initiation of washout. When there is no adsorption, the adsorption index would be 0. Values are mean ± s.e.m. of six microelectrodes. The values of dopamine (1.0 μM) and also DOPAC (10 μM) are presented.

3.2. Validation by stimulation-evoked dopamine release

The capability of *in vivo* dopamine detection was evaluated in the mouse striatum (Fig. 5). Pairs of diamond microelectrodes and carbon fibres were implanted in parallel into the striata of anaesthetized mice ($n = 3$). As compared to the previous study using pulse-voltammetry (Suzuki et al., 2007), the sensitivity was much improved during constant-current amperometry on the diamond microelectrode. The peak amplitude to the MFB stimulus of 12 pulses at 30 Hz was 0.33 (±0.10) nA, with a S/N ratio of 23.3 (±12.6) with the diamond microelectrode amperometry, whereas 20.45 (±6.43) nA with a S/N ratio of 43.7 (±20.9) with carbon fibre FSCV ($n = 3$, mean ± s.e.m.). This result indicates that the actual limit of detection of the diamond microelectrode *in vivo* detection was comparable to that of the carbon fibre.

The dopamine uptake inhibitor nomifensine enhanced the amplitude of dopamine release, consistent with a former study (Oyama et al., 2010), indicating the evoked response after the stimuli is mediated primarily by dopamine (Fig. 5B). After the effect of nomifensine was stabilized, amperometry and FSCV were used to test both carbon fibre and diamond microelectrodes (Fig. 5C). The temporal patterns of both microelectrodes were similar upon amperometric measurement, suggesting equivalent diffusion time from the synaptic terminals to the electrode surface (Cragg and Rice, 2004). The response of FSCV on diamond microelectrodes was similar to that obtained with amperometry, whereas FSCV on carbon fibres provided results with a broader range than amperometry at the same electrode.

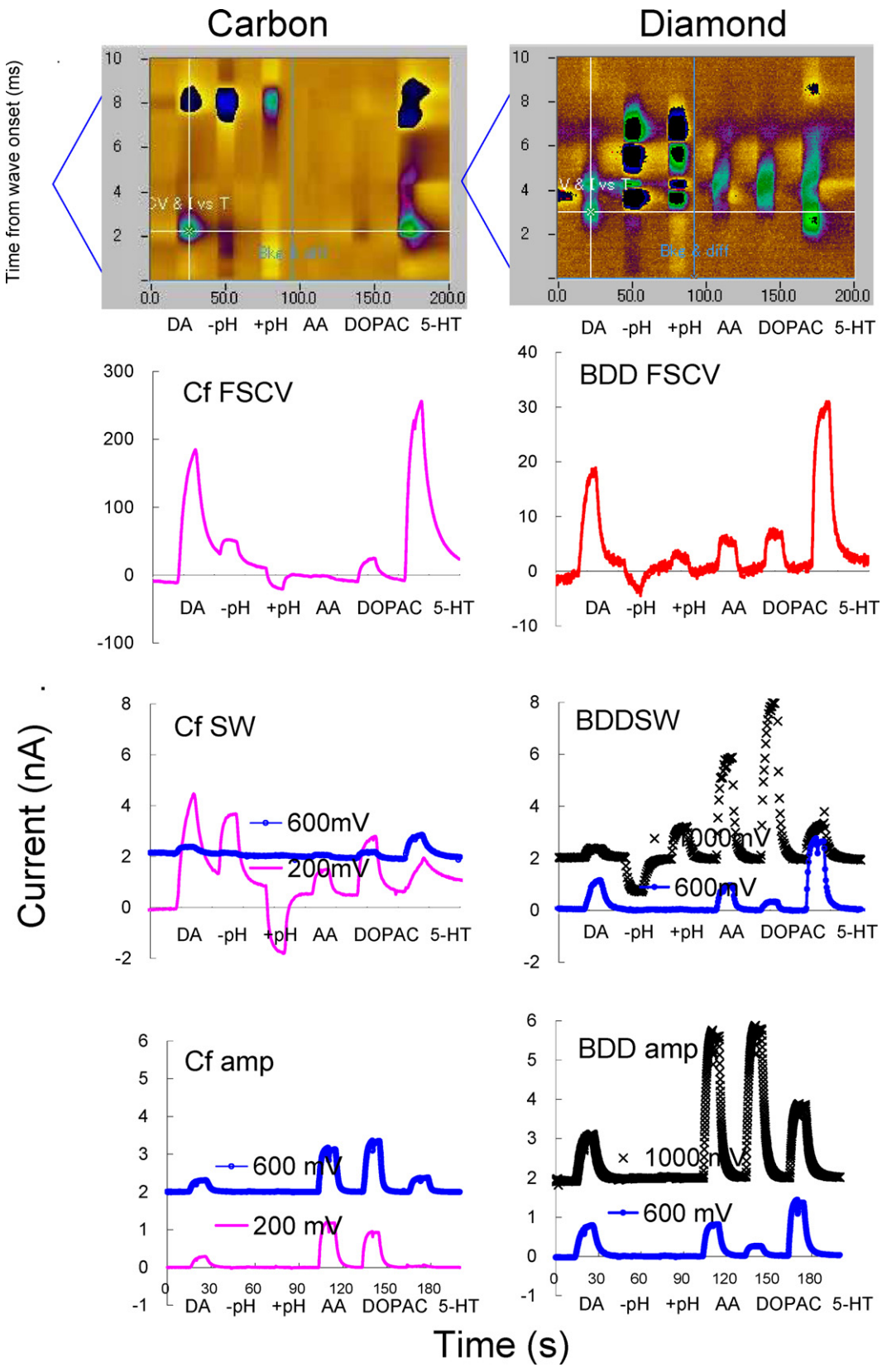

Fig. 3. *In vitro* electrochemical recordings on carbon-fibre (Cf, left) and diamond microelectrodes (BDD, right). Three types of recordings, FSCV (the first and second top), SW (second bottom), and constant-potential amperometry (bottom). The microelectrode tips were placed in a flow of pH 7.4 PBS and switched to the test solutions of 1 μM dopamine (DA), PBS pH 7.2 (−pH), PBS pH 7.6 (+pH), 10 μM ascorbate (AA), 10 μM DOPAC and 1 μM 5-HT. The top is the colour-plot of background-subtracted FSCV, and the white horizontal line indicates the potential shown in the second-top chart. The background was defined at the blue vertical line. For SW and amperometry, the results at two representative potentials are presented (magenta bold line: 200 mV, blue circle: 600 mV, and black cross: 1000 mV). The baseline of the higher potential was vertically shifted by 2 nA. (For interpretation of the references to colour in this figure legend, the reader is referred to the web version of the article.)

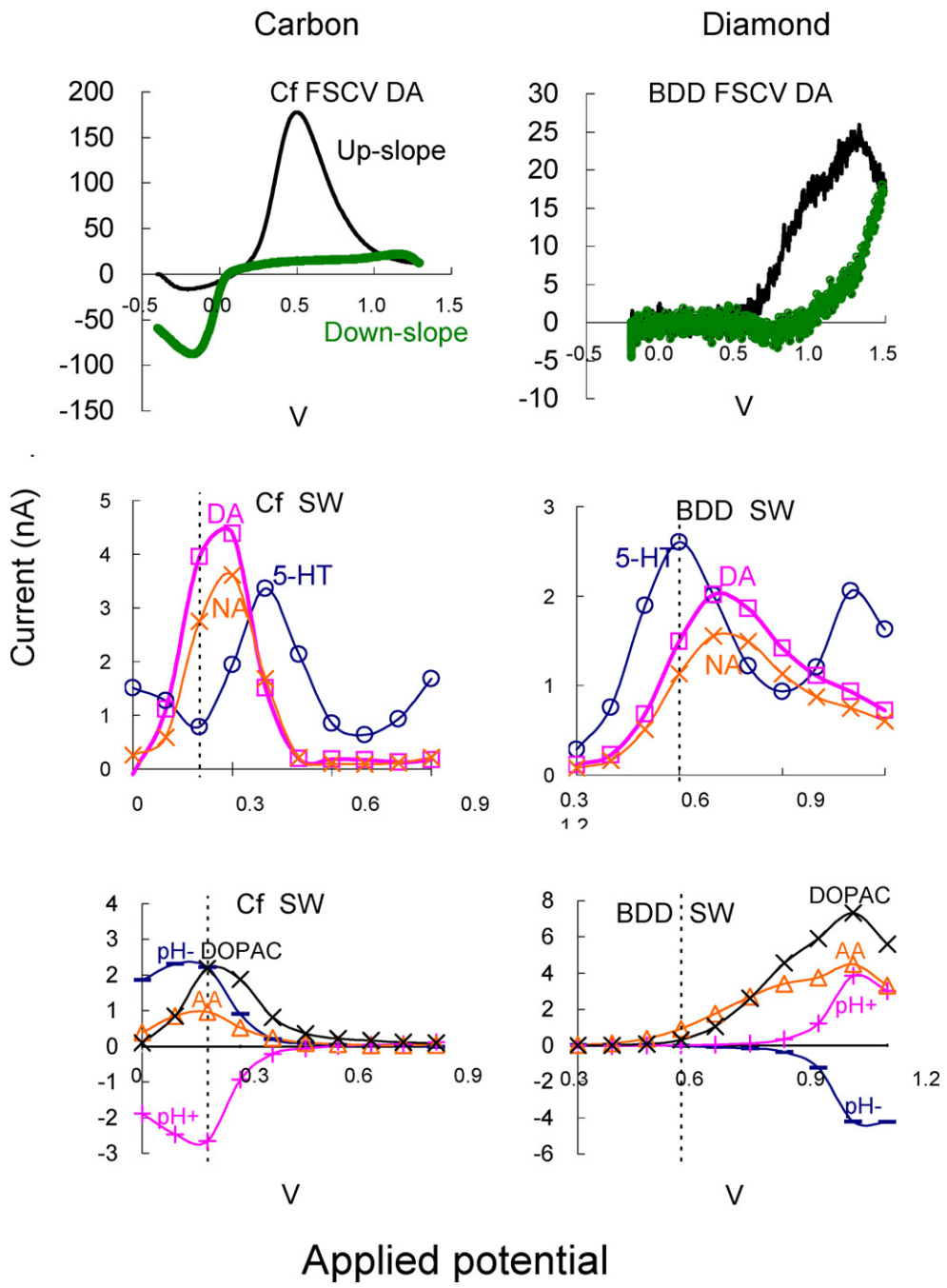

Fig. 4. Voltage dependency *in vitro*. Left: carbon and right: diamond. Top: Background-subtracted cyclic voltammograms at FSCV (black: oxidation phase of upslope, green: reduction phase of downslope). Middle and bottom: voltage-dependency of SW. middle: monoamines; bottom: other test chemicals. Magenta square: dopamine, orange cross: noradrenaline, blue circle: 5-HT, blue horizontal bar: pH 7.2, magenta plus: pH 7.6, orange triangle: ascorbate, black cross: DOPAC. (For interpretation of the references to colour in this figure legend, the reader is referred to the web version of the article.)

Electrical stimulation was also delivered to the monkey MFB. The tip of a tungsten electrode was placed just dorsal to the STN, and the amperometric current response to a 60-Hz stimulus was detected in the striatum (Fig. 5D). The response current in the monkey brain was relatively low, presumably because the stimulation was delivered by only one electrode, whereas a twin parallel electrode was used in mice. Also, the stimulation position for monkey MFB may not yet be optimized. The amplitude of MFB responses in mice depends strongly on fine adjustment of the stimulation positions. At present, we could not confirm whether the effective stimulation was given in MFB or STN because STN stimulation can also evoke dopamine release in the striatum (Shon et al., 2010).

3.3. Reward responses in the monkey striatum

Figs. 6 and 7 show amperometric recordings by the diamond microelectrode in the monkey caudate during a Pavlovian task. Monkey S received juice reward 2 s after the light cue, whereas the interval was 1 s for monkey K. Three sessions of monkey S and seven of monkey K are summarized in Table 3. The behavioural schedule was first changed step by step in monkey S, whereas three kinds of trials were systematically applied in monkey K.

Simple juice response (S3): In the early session of monkey S (S3) testing, juice was delivered without a preceding cue. The juice valve was opened for 250 ms at first, and in the subsequent portion of the experiment, the juice valve was opened three times at 2 Hz (orange

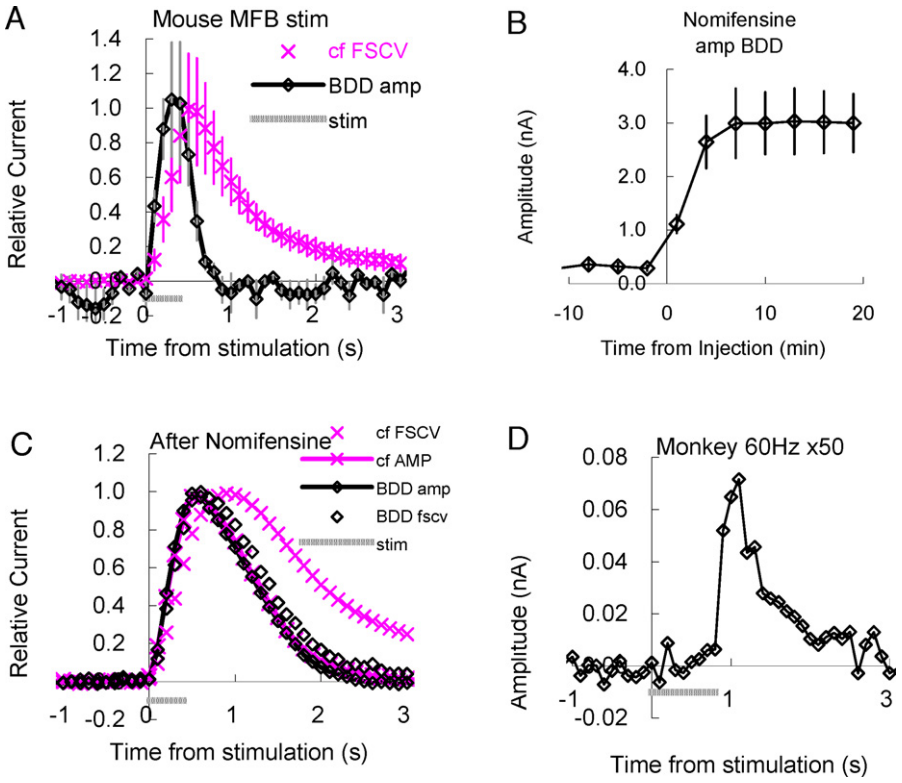

Fig. 5. *In vivo* recording of evoked dopamine release. (A) Electrochemical recordings in the mouse dorsal striatum were made as shown in Fig. 1D. Electrical stimulation of 12. pulses at 30 Hz (grey bold line) was given to the nigro-striatal tract (MFB). The averaged currents of three mice obtained using FSCV on carbon fibre (cross, −0.4 to 1.3 V) and amperometry on the diamond microelectrode (open diamond with bold line, +600 mV) are shown, after normalization to peak amplitude. (B) The effect of a dopamine uptake inhibitor on evoked dopamine release. The MFB stimulation was repeated every 3 min during amperometric recordings on the diamond microelectrode. Nomifensine (7 mg/kg, s.c.) was injected at time 0. (C) Comparison of *in vivo* recordings on carbon fibre (cf) and diamond (BDD) microelectrodes using FSCV and amperometry (magenta cross: FSCV on cf, black open diamond: FSCV on BDD, magenta cross with line: amperometry at +200 mV on cf, black open diamond with line: amperometry at +600 mV on BDD). These recordings were made following the nomifensine administration shown in B, where the selectivity and the amplitude of evoked dopamine release were maximized. For FSCV, the representative potential was chosen to maximize the evoked response. (D) MFB response in the monkey caudate (amperometry at +600 mV on BDD). Electrical stimulation (60 Hz, 50 pulses) was delivered to the dorsal border of subthalamic nucleus (STN). An average of three traces is presented. (For interpretation of the references to colour in this figure legend, the reader is referred to the web version of the article.)

horizontal lines in Fig. 6B). The animal did not stay very calm during this session, but after the trials were selected according to the rule described above, the remaining 16 trials showed a clear response after the juice onset (time effect: $F_{(19,285)} = 2.56$, $p < 0.001$; one-way repeated measures ANOVA for S3, 20 points from −0.3 to 1.6 s, $n = 16$ Juice trials) (Fig. 6B). There was no difference between one and three valve openings (valve schedule effect: $F_{(1,14)} = 0.37$, $p = 0.552$, valve schedule × time interaction: $F_{(19,266)} = 0.632$, $p = 0.695$; two-

Table 3
Summary of amperometric measurement during behavioural task.

Session	Electrode and calibration			Trial number					Temporal analysis of paired trials				
	Electrode	Pre nA/	Post 1 μMDA	Total	P	L	J	Excluded	Amplitude (pA)	*F*	*p*	Increased timing (s from cue onset)	
Monkey S													
S3	B7	1.20	0.32	54	–	–	16	38	–				
S7	f193	1.30	0.74	69	33	23	11	2	55.8	$F(40,1280) = 22.38$	<0.01	0.12–0.20	2.12–2.20
S8	f193	1.30	0.80	48	34	7	–	7	15.5	$F(40,1320) = 4.31$	<0.01	0.20	–
Total				117	67	30	11	9		$F(40,2640) = 19.32$	<0.01	0.12–0.20	2.12–2.20
Monkey K													
K6	f193	2.15	2.05	48	22	13	11	2	74.1	$F(40,840) = 4.34$	<0.01	0.36	–
K10	j5	0.72	0.34	30	11	9	7	3	3.6	$F(40,400) = 1.35$	ns	–	–
K11	j5	1.22	0.41	70	36	18	14	2	29.6	$F(40,1400) = 4.19$	<0.01	0.28–0.36	–
K15	kj3	0.85	0.30	50	28	8	9	5	3.7	$F(40,1080) = 2.43$	<0.01	–	–
Total				198	97	48	41	12		$F(40,4720) = 5.29$	<0.01	0.28–0.36	–
Excluded sessions for low sensitivity													
S6	f193	0.88	–	160	86	62	–	12	14.3	$F(40,3400) = 9.00$	<0.01	0.12	–
K7	f196	0.93	0.15	50	22	15	10	3	3.1	$F(40,840) = 0.92$	ns	–	–
K12	j1	1.85	–	70	34	15	12	9	7.6	$F(40,1320) = 1.37$	ns	–	–
K13	j4	4.50	–	60	32	13	9	6	5.3	$F(40,1240) = 2.46$	<0.01	–	–

Left: *in vitro* calibration just before and after *in vivo* measurement. "–" indicates that the electrodes lost sensitivity to dopamine. Middle: Trial numbers for each session. P: paired, L: light-without-juice, J: juice without-light trials. Right: one-way ANOVA analysis of paired trials. When the post-recording sensitivity was less than 0.3 nA/μM (S6, K7, K12, and K13), the result was not included for the population data (Figs. 6D and 7C). Experimental sessions designed to record the other brain regions and sessions which are plagued by apparent technical failures are not included in the table. Time points significantly larger ($p < 0.05$, Tukey HSD) than any of four points before the initiation of light stimulation are indicated.

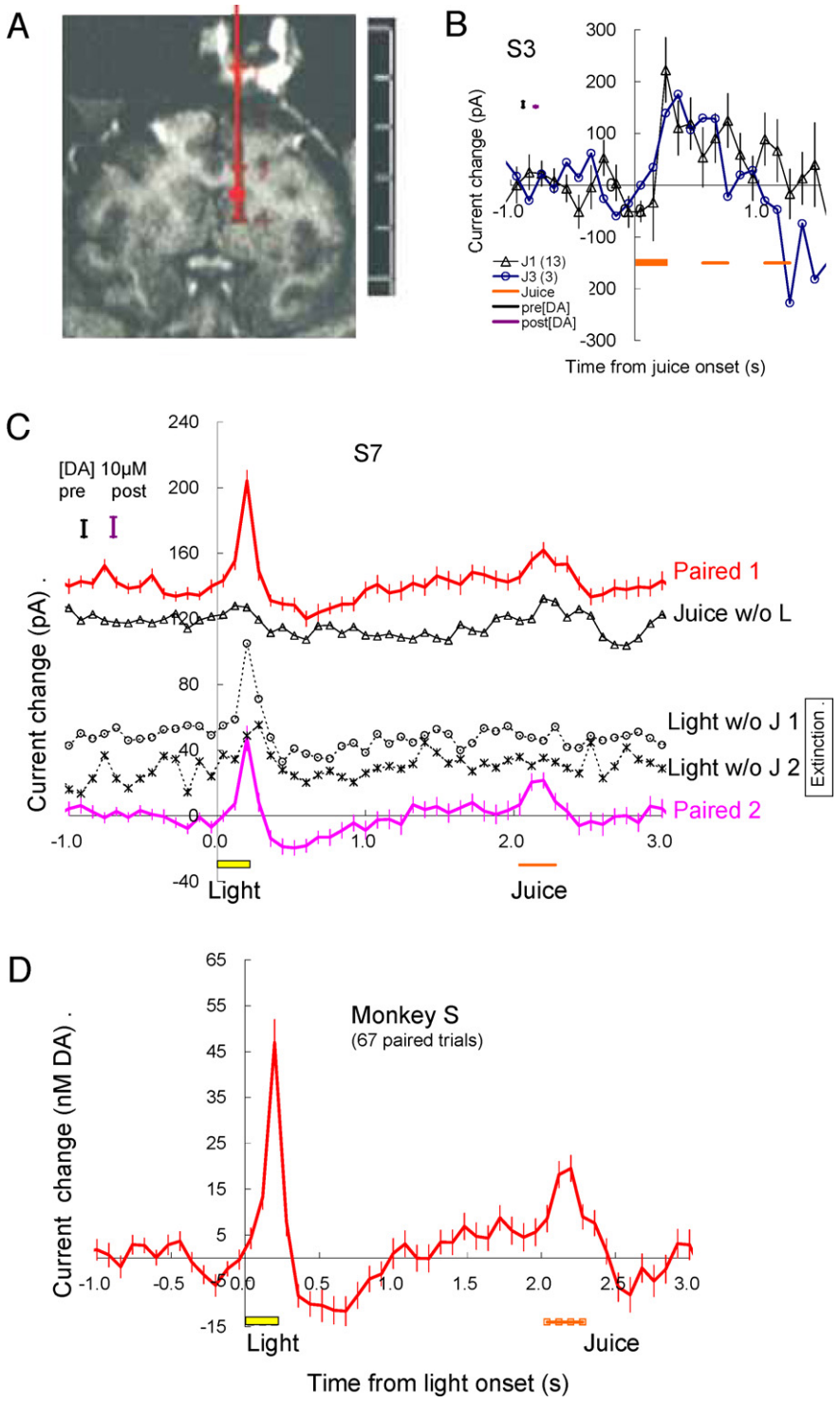

Fig. 6. *In vivo* recording in the caudate of monkey S during the behavioural tasks. Amperometric recordings at +600 mV on diamond microelectrodes. (A) MRI image with the estimated electrode position. (B) Session S3 with only juice deliveries. The ordinate axis represents average current ± s.e.m. (pA). Time 0 is aligned to the onset of the juice (orange line). In the early half of the session S3, the juice valve was opened once for 250 ms for 0.5 ml of juice (J1, black triangle), whereas the valve was opened three times in the later half (J3, blue circle). More details are provided in Table 3. (C) Pavlovian task in session S7. Time 0 is aligned to the onset of the light cue (yellow squares), and the juice (orange line) was delivered 2.0 s later. Three types of trials, paired (P1 and P2, red bold line), juice-without-light (J, black triangles with black line), and light-without-juice (L1 and L2, black circle and asterisk with dotted line) are presented. For simplification, s.e.m. was indicated only for Paired trials, and the baselines are vertically shifted. The two vertical lines on the left indicate the current intensity for 10 nM dopamine in the *in vitro* calibrations, just before (left, black) and after (right, purple) the recording. (D) Pooled data for all paired trials. The ordinate axis indicates estimated dopamine concentrations (nM). (For interpretation of the references to colour in this figure legend, the reader is referred to the web version of the article.)

way repeated measures ANOVA for S3, 20 points from −0.3 to 1.6 s, $n = 13$ one-opening, $n = 3$ three-openings) (Fig. 6B). The three-valve trials showed that the subject responded only to the initiation of the reward event, but not to each individual valve opening. The result demonstrated that it was a response to a single rewarded event. The lack of specific responses to the second and third valve openings indicates the current response was not derived from the switching noise but rather from some behavioural consequence.

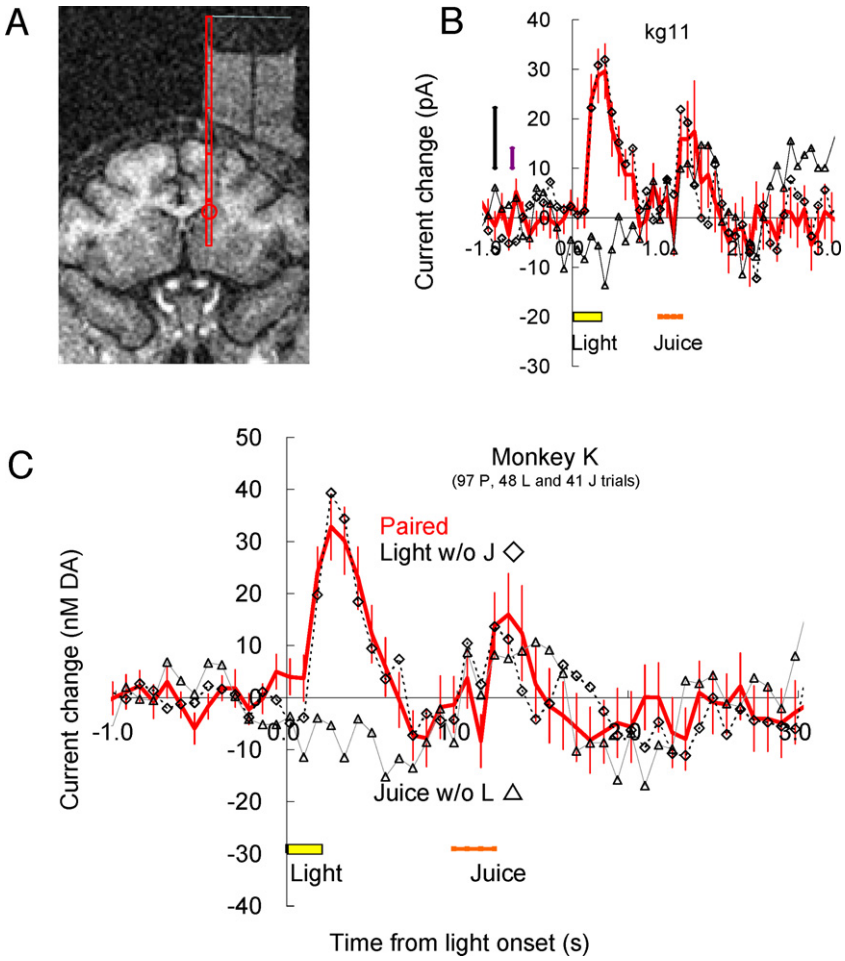

Fig. 7. *In vivo* recording in the caudate of monkey K during the behavioural tasks. (A) MRI image with the estimated electrode position. (B) A successful session with monkey K. The juice (orange line) was delivered 1.0 s after the light onset (yellow squares). Unlike monkey S, three types of trials, paired (P, red bold line), light-without-juice (L, black circle with dotted line) and juice-without-light (J, black triangles with black line) were shuffled in a pseudo-random sequence. (C) Pooled data for all trials. Details of the presentation are the same as in Fig. 6. (For interpretation of the references to colour in this figure legend, the reader is referred to the web version of the article.)

Pavlovian paired conditioning: Although 10 Hz sampling was used in session S3, the sampling rate was improved to 25 Hz in later sessions. In addition, a 2-s preceding light cue was paired to juice delivery (Fig. 6C and D). In one session (S7, Fig. 6C), clear current responses to the light cue were observed. The temporal changes of all light-juice paired (P) trials were significant (time effect: $F_{(40,1280)} = 22.38$, $p < 0.001$; one-way repeated measures ANOVA for S7, 41 points from −0.28 to 2.92 s, $n = 33$ paired trials) (Fig. 6C and Table 3), and a significant increase of the current was detected 0.12–0.20 s and 2.12–2.20 s after cue onset (Tukey's HSD test, difference from the pre-event points from −0.28 to −0.04 s, $p < 0.05$).

To evaluate the behavioural significance of the amperometric current responses, juice without light (J) trials and light without juice (L) trials were introduced during the session (S7).

Light reponses (S7): Session S7 was separated into two parts, before and after an extinction procedure. During the early half of the session, the light was intermittently shaded with cardboard in a shuffled sequence (Juice w/o Light: J trials, black triangles in Fig. 6C). The light response was absent when the light was not visible (vision × time interaction: $F_{(19,494)} = 5.33$, $p < 0.001$; two-way repeated measures ANOVA for the 17 Paired and 11 Juice trials, 20 points from −0.28 to 1.24 s).

During the latter half, the juice tube was manually closed for 23 trials (Light w/o Juice; L1: $n = 11$ and L2: $n = 12$) to see the effect of extinction, and then the tube was re-opened to recover the association between the light and the juice reward (Paired 2: $n = 16$, Fig. 6C). The peak after the light timing remained in the first 11 trials (L1) but dropped during the later 12 trials (L2) and recovered in the following paired trials (Paired 2). A two-way repeated measures ANOVA showed that the task × time interaction was significant ($F_{(38,684)} = 1.81$, $p = 0.040$; 20 time points from −0.28 to 1.24 s). The lower light response during L2 and the recovery during P2 indicate that the light response depended on the association of light and juice delivery.

Juice responses (S7): The response to juice delivery was lower than the light responses but also reflected task conditions (task × time interaction: $F_{(38,1216)} = 2.28$, $p = 0.002$; two-way repeated measures ANOVA for S7, 20 points from 1.72 to 3.24 s, $n = 33$ Paired trials, $n = 23$ Light trials, $n = 11$ Juice trials) (Fig. 6C). When the trials with or without juice were compared directly, the difference was also significant (juice × time interaction: $F_{(19,1026)} = 3.36$, $p = 0.001$; two-way repeated measures ANOVA for S7, 20 points from 01.72 to 3.24 s, $n = 33$ Paired trials, $n = 23$ Light trials; the difference between Paired and Light was significant at 2.20 s) (Fig. 6C). This result indicates that the peak after juice onset was actually dependent on juice delivery. During these juice without light (J) trials and light without juice (L) trials, the light and juice were omitted manually and no change was made on the computer-controlled light and juice valve operations. Although constant-potential amperometry is inherently susceptible to noise

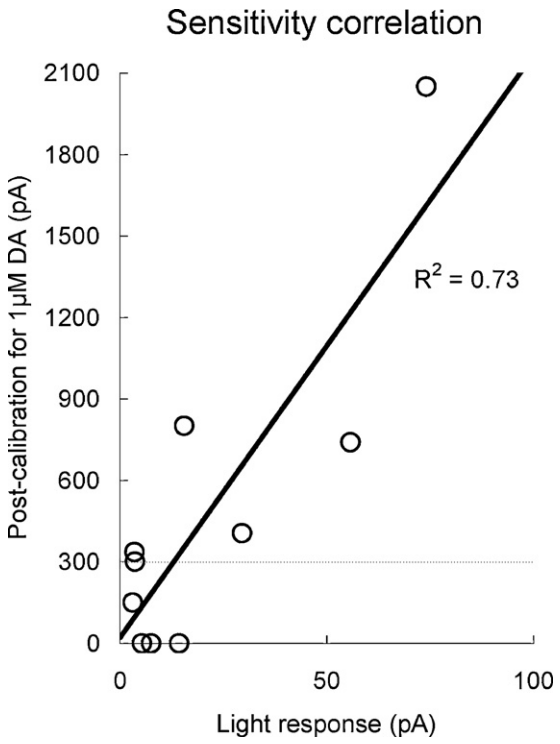

Fig. 8. Correlation between the *in vivo* amplitude of light response and *in vitro* sensitivity to dopamine after removal from the brain.

artefacts, these results of J and L trials indicate that the current responses reflected some biological brain responses.

Endurance of diamond microelectrodes in the brain: After each measurement, the diamond microelectrodes used were calibrated with dopamine solutions. Vertical bars indicate amplitude corresponding to 10 nM dopamine before and after the *in vivo* measurement (Figs. 6, 7 and Table 3). The sensitivity of diamond microelectrodes was maintained during *in vivo* recording of K6 (Table 3), consistent with the reported endurance of diamond electrodes against bio-fouling (Trouillon and O'Hare, 2010), but the sensitivity deteriorated in some sessions (Table 3). The peak amplitude after the cue and post-calibration correlated significantly ($r = 0.85$, $n = 10$, $p < 0.01$), suggesting that the measured current responses reflected dopamine concentrations (Fig. 8). To detect a significant response, at least 0.3 nA/μM sensitivity to dopamine seems to be required for a meaningful *in vivo* measurement (Table 3, Fig. 8). For this reason, sessions of S6, K7, K12 and K13 were not included for the further analysis (Table 3).

Population data for Monkey S: To pool the results from different recording sessions, the dopamine concentration was estimated using the calibration value after the *in vivo* measurement. The paired trials from sessions S7 (Fig. 6C) and S8 (Suppl. 2) of monkey S were pooled as the dopamine concentration, and the temporal change was significant (time effect: $F_{(40,2640)} = 19.60$, $p < 0.001$; one-way repeated measures ANOVA for pooled S7 and S8, 41 points from −0.28 to 2.92 s, $n = 67$ Paired trials) (Fig. 6D). A significant current increase was detected after the light cue at 0.12–0.20 s and after the juice delivery at 2.12–2.20 s (HSD test, $p < 0.05$).

Population data for Monkey K: Similar results were obtained in the second monkey, K (Fig. 7, Suppl. 2 and Table 3). In monkey K, the task was modified in two ways. First, three types of trials (Paired, L and J) were systematically presented in a shuffled sequence with ratios of either 6:2:2 or 5:3:2. Second, the interval between light and juice was shortened to 1.0 s. The pooled data from paired trials for monkey K revealed a main effect of time (time effect: $F_{(40,3840)} = 6.34$, $p < 0.001$; one-way repeated measures ANOVA for pooled K, 41 points from −0.28 to 2.92 s, $n = 97$ Paired trials) (Fig. 7C, red). A significant current increase was detected after the light cue at 0.28–0.36 s (HSD test, $p < 0.05$). The effect of light was detected (task × time interaction: $F_{(38,3458)} = 3.59$, $p < 0.001$; two-way repeated measures ANOVA for pooled K, 20 points from −0.28 to 1.24 s, $n = 97$ Paired trials, $n = 47$ Light trials, $n = 41$ Juice trials, significant group differences from 0.20 to 0.52 s) (Fig. 7C). A significant effect was not found after juice delivery at 1 s (task × time interaction: $F_{(38,3458)} = 1.01$, $p = 0.436$; two-way repeated measures ANOVA for pooled K, 20 points from 0.68 to 2.20 s, $n = 97$ Paired trials, $n = 47$ Light trials, $n = 41$ Juice trials) (Fig. 7C).

4. Discussion

In the present study, we applied electrochemistry with a novel diamond microelectrode and successfully detected sharp transient current changes in the mouse and monkey striatum. Diamond microelectrodes were suitable for constant-potential amperometry, which was sensitive enough for *in vivo* dopamine detection. This technique discriminated dopamine release from pH changes (Fig. 3 bottom) and facilitated penetration into the deep part of large brains. During *in vivo* recordings, sharp current increases were evoked by stimulation of the nigrostriatal tract, which was enhanced by a dopamine uptake inhibitor (Fig. 5B).

4.1. Comparison of amperometry and FSCV

We adopted constant potential amperometry for the diamond microelectrode because it was the most sensitive method for the detection of dopamine. The diamond microelectrode had poor sensitivity to dopamine on FSCV, although the waveform may not have been optimized for the diamond microelectrode. This poor sensitivity may be due to less adsorption on the diamond electrode, which contributes to the high sensitivity of FSCV at carbon fibres (Bath et al., 2000; Venton et al., 2002; Heien et al., 2003). Another possibility is its slow electrochemical transfer. In the dopamine response to a pulse (Fig. 2, green line), the dopamine oxidation current appears slower than the carbon fibre.

The temporal resolution of amperometry was superior to that of FSCV. The FSCV on carbon fibre has been questioned by some researchers with regard to its temporal resolution (Schultz, 2007; Venton et al., 2002). The temporal skewness was less with amperometry because its adsorption was less than that of FSCV. In addition, the temporal resolution of FSCV is limited by the time of voltage cycles; with amperometry, data sampling can be much more frequent, because there are no cycles.

Diamond microelectrodes were sensitive to the pH changes at higher potential (Fig. 4 bottom-right), consistent with previously obtained results (Mitani and Einaga, 2009). Interestingly, the direction of current in response to acidic or basic pH conditions opposed that observed with the carbon fibres (Fig. 4 bottom), suggesting a different mechanism from that of carbon fibres.

Although constant potential amperometry has better temporal resolution (Dommett et al., 2005), it is not suitable for identifying multiple electrochemical factors due to the lack of "voltage signatures" (Heien et al., 2004). Whereas principal component regression analysis can extract dopamine-like component from original FSCV data (Heien et al., 2004), it is not applicable to constant-potential amperometry. On the other hand, it is worth noting that amperometry does not react to pH changes, which is the main distractor of dopamine signals detected by FSCV with carbon fibres.

Because the electrochemical reaction of monoamines requires the lowest potential on diamond (Fig. 4 middle), the influence of other electrochemical factors is minimized by keeping the voltage below the responsive potential of these additional factors

(Figs. 3 and 4). Importantly, in agreement with former observations (Nakazato and Akiyama, 1999; Hashemi et al., 2009; Rodríguez et al., 2007), carbon fibres held at 200 mV can detect dopamine without interference from 5-HT (Fig. 3 bottom, Cf-amp). In the case of FSCV on diamond microelectrodes, the foot of the intense pH response overlapped with that of dopamine (Fig. 3 up-right). Therefore the lack of a voltage-signature in constant-potential amperometry does not necessarily indicate poor chemical resolution.

In summary, compared with the widespread use of FSCV on carbon fibres, amperometric recording on diamond microelectrodes has three advantages: (1) less temporal skew by adsorption (Fig. 3, Table 2), (2) minimal influence by pH changes (Fig. 3 bottom-right), and (3) easy handling for penetration into the deep part of large brains. By contrast, our method has three disadvantages: (1) it can be influenced by ascorbate and DOPAC (Fig. 3 bottom-right), (2) the absolute current is low and easily influenced by various sources of noise including animal movements, and (3) sensitivity *in vivo* can deteriorate (Table 3).

4.2. Reward responses in the monkey brain

In this study, we recorded significant current changes associated with behavioural context. In the S3 session, positive current response followed juice delivery (Fig. 6B). It is interesting that there was only one response after the first valve opening when the valve was opened three times. We hypothesize that the monkey has learned that the first valve opening is predictive of three openings and served as a conditioned stimulus for three liquid rewards. In the Pavlovian tasks, when a preceding light cue was paired to the juice, a sharp current response followed the light cue. During the S7 session (Fig. 6C), the light response was low when the light was not visible (Juice w/o Light: J) and also when the juice reward did not follow the light ('Light w/o Juice' -2). The current responses after juice delivery were lower than the light response but disappeared when juice delivery was stopped (Light w/o Juice: L). These results indicate that the recorded current response was associated with certain behavioural contexts.

4.3. Was the reward response dopaminergic?

Although we intended to detect dopamine release in the monkey brain and recorded current responses to the reward prediction cue, our results are not sufficient to conclude that we have "specifically" measured dopamine release in the monkey brain. Unlike microdialysis, chemical identification cannot be definitive in *in vivo* voltammetry using microprobes inserted directly in the brain. Both FSCV on carbon fibres and our method cannot distinguish NA from dopamine (Fig. 4 and supplemental Fig. Suppl. 1). Proper selection of the electrode and recording technique depend on the particular subject of the study. For instance, FSCV on the carbon fibres should be used if differentiation from ascorbate is important, and constant potential amperometry on diamond microelectrode is preferable when differentiation from pH and/or temporal resolution is important. It may even be better to place several microelectrodes in one brain and apply several electrochemical techniques in parallel (Agnesi et al., 2009; Zachek et al., 2009).

A number of criteria have been suggested for correct identification of the chemical giving rise to *in vivo* voltammetric signals (Marsden et al., 1988): (1) reasonable magnitude of the response corresponding to the estimated tissue concentrations, (2) separation of the specific chemical from other electroactive chemicals in the brain, (3) identity of electrochemical peak for the compound considered, (4) anatomical specificity, (5) effect of substrate-specific enzymes and (6) pharmacological interventions, and finally (7) general agreement with measurements obtained using other methods.

For criterion (1), the amplitude of reward-related responses are within the order of 100 nM in the studies using FSCV on carbon fibres in rodents. The amplitude of our result in the monkey brain was within this range.

For criterion (2), amperometry on a diamond microelectrode can separate pH from dopamine but is not very selective with respect to ascorbate, DOPAC and other monoamines (Figs. 3 and 4). However, the short latency and duration of the responses do not match the time courses of metabolic changes of ascorbate or DOPAC, which would occur in the range of 1 s or more. The first peak current within 1 s after MFB stimulation is thought to be caused by dopamine release (Heien et al., 2004). In addition, the monoamine tissue concentration in the rostral caudate of intact macaque monkey was 7869 ng/g tissue for dopamine, 31 ng/g for NA, and 232 ng/g for 5-HT, whereas the dopamine concentration of cerebral cortex was less than 100 ng/mg (Pifl et al., 1991). The extremely high concentration of dopamine in the monkey caudate suggests that dopamine is most likely to contribute to the major part of the response (Brown et al., 1979; Di Paolo et al., 1986; Gerhardt et al., 1996), similar to the results observed in rodents (Rollema et al., 1989; Willis et al., 1988).

For criterion (3), we have shown a necessary condition of voltammetric identity, i.e., the detection of the reward response at the same potential sensitive to dopamine. Also, the amplitude of the cue responses correlated to the dopamine sensitivity after removal from the brain (Table 3 and Fig. 8). It is possible that the experiments were repeated using a potential applied to the electrode that was insufficient to oxidize dopamine (e.g., 0 mV vs. Ag/AgCl).

Criterion (4) should be qualified if the recording was made not only in caudate, but also in a brain area with few dopamine terminals, such as white matter. These techniques should be applied in future studies to support the molecular identification necessary for criteria (3) and (4). The pharmacological interventions suggested in (5) and (6) should also be verified in the monkey brain because the effect of nomifensine has only been confirmed in mice (Fig. 5B). At present, the results shown in Figs. 4 and 5 seem to satisfy criterion (7) and are in general agreement with the known phasic responses of the temporal characteristics, which are consistent with those of midbrain dopamine neuron excitation (Joshua et al., 2008; Fiorillo et al., 2003; Matsumoto and Hikosaka, 2009; Schultz et al., 1993, 1997; Schultz, 2007; Takikawa et al., 2004).

Additional verification is awaited, but by fulfilling the (1), (2) and (7) criteria, it may not be too speculative to suggest that the current peaks recorded reflect dopamine release induced by the reward cue.

4.4. Overcoming species differences

Phasic reward-induced dopamine release in the striatum has been successfully detected using FSCV in behaving rodents (Day et al., 2007; Natori et al., 2009; Phillips et al., 2003; Roitman et al., 2004; Wanat et al., 2010). In these studies, the dopamine responses to the cue did not exceed those of reward retrieval. Recently, Flagel et al. (2011) revealed that the cue/reward ratio of dopamine responses can differ even among sub-strains of Sprague–Dawley rats. Larger difference is expected between rodents and primates. Voltammetric measurement of dopamine release has mainly been studied in rodents and reward-induced impulse activity of midbrain dopamine neurons has mainly been studied in primates. Because of this, it is important to consider species differences, before discussing the potential discrepancy of dopamine release and midbrain impulse activities. In this study, we have developed a method to measure dopamine releases in the monkey brain, which

has made it possible to compare both measurements in the same monkey.

The consistency and differences of striatum between animal groups have been studied in several comparative studies (Björklund and Dunnett, 2007; Graybiel, 1995; Voorn et al., 2004; Schultz, 2007). There are considerable differences in striatum structure between primates and rodents (Voorn et al., 2004; Björklund and Dunnett, 2007). In primates, the caudate and putamen are separated, whereas there is no anatomical boundary between lateral and medial striatum in rodents. The anatomical location of the measurement can result in functional differences in dopamine neurotransmission (Cragg et al., 2002; Phillips et al., 2002; Garris et al., 1994; Wickens et al., 2007; Yavich, 1996; Zhang et al., 2009). Moreover, the role of striatal dopamine in motor control differs between rodents and primates. Dopamine deprivation and striatal lesions induce Parkinsonism in primates but results in subtle or no motor deficits in rodents (Di Paolo et al., 1986; Kishioka et al., 2009; Rollema et al., 1989; Shiotsuki et al., 2010; Willis et al., 1988). On the other hand, the differences and consistency of reward responses are not very clear. For these reasons, it is hard to reconcile the reported knowledge of electrical and chemical dopamine responses, because such data may include both species differences and discrepancies between detection methods. For a more generalized understanding of the dopaminergic reward system, it is necessary to utilize the same task for the same animals to obtain meaningful comparisons.

We recorded phasic reward prediction responses in the striata of behaving primates, although further verification of chemical selectivity is awaited. This method can open new directions for future studies. First, this method could be useful in comparing time courses of dopamine release and uptake in various areas of the monkey forebrain. The medial and lateral parts of midbrain dopaminergic neurons exhibit different responses to negative rewards (Matsumoto and Hikosaka, 2009). In general, the transfer function at chemical neurotransmission at the synaptic terminal is non-linear. Because the kinetics of extracellular dopamine differ among projection areas (Cragg and Rice, 2004; Cragg et al., 2002; Garris et al., 1994; Phillips et al., 2002; Yavich, 1996; Wickens et al., 2007; Zhang et al., 2009), actual release data obtained at each forebrain area are essential to establish brain models of reinforcement learning.

Second, simultaneous recording of reward response of striatal tonically active neurons (TAN) and local dopamine release will be possible. TAN cholinergic neurons also transmit reward information in the striatum (Joshua et al., 2008), but the roles of the dopamine and TAN neurons are not well understood. Voltammetric studies have already revealed the modulation of dopaminergic terminals by nicotinic acetylcholine receptors in brain slices (Rice and Cragg, 2004; Zhang et al., 2009). Functional study of these neurons is only possible in the striatum of behaving monkey. In addition to acetylcholine, dopamine itself modulates its release via dopamine D2 autoreceptors (Cragg and Greenfield, 1997; Phillips et al., 2002; Schmitz et al., 2003). These modifications in the terminals of dopamine projections can be studied in primates by using the method introduced in the present study.

Acknowledgements

The authors thank Ms. Yukiko Abe, Mr. Tomoa Kamizono and Dr. Tetsuji Ochiai for their help in the experiments and Dr. Taizo Nakazato for electrochemical equipment.

Grants: This work was supported in part by the Strategic Research Program for Brain Sciences (SRPBS) and a Grant-in-Aid for Scientific Research on Priority Areas "Emergence of Adaptive Motor Function through Interaction between Body, Brain and Environment (Mobiligence)" from the Japanese Ministry of Education, Culture, Sports, Science and Technology (MEXT).

Disclosures: We have nothing to disclose.

Appendix A. Supplementary data

Supplementary data associated with this article can be found, in the online version, at doi:10.1016/j.neures.2011.05.013.

References

Abeliovich, A., Schmitz, Y., Farinas, I., Choi-Lundberg, D., Ho, W.H., Castillo, P.E., Shinsky, N., Verdugo, J.M., Armanini, M., Ryan, A., Hynes, M., Phillips, H., Sulzer, D., Rosenthal, A., 2000. Mice lacking alpha-synuclein display functional deficits in the nigrostriatal dopamine system. Neuron 25, 239–252.

Agnesi, F., Tye, S.J., Bledsoe, J.M., Griessenauer, C.J., Kimble, C.J., Sieck, G.C., Bennet, K.E., Garris, P.A., Blaha, C.D., Lee, K.H., 2009. Wireless instantaneous neurotransmitter concentration system-based amperometric detection of dopamine, adenosine, and glutamate for intraoperative neurochemical monitoring. J. Neurosurg. 111, 701–711.

Bard, A.L., Faulkner, L.R., 2002. Electrochemical Methods: Fundamentals and Applications, 2nd ed. John Wiley and Sons.

Bath, B.D., Michael, D.J., Trafton, B.J., Joseph, J.D., Runnels, P.L., Wightman, R.M., 2000. Subsecond adsorption and desorption of dopamine at carbon-fiber microelectrodes. Anal. Chem. 72, 5994–6002.

Brown, R.M., Crane, A.M., Goldman, P.S., 1979. Regional distribution of monoamines in the cerebral cortex and subcortical structures of the rhesus monkey: concentrations and *in vivo* synthesis rates. Brain Res. 168, 133–150.

Björklund, A., Dunnett, S.B., 2007. Dopamine neuron systems in the brain: an update. Trends Neurosci. 30, 194–202.

Cragg, S.J., Greenfield, S.A., 1997. Differential autoreceptor control of somatodendritic and axon terminal dopamine release in substantia nigra, ventral tegmental area, and striatum. J. Neurosci. 17, 5738–5746.

Cragg, S.J., Hille, C.J., Greenfield, S.A., 2002. Functional domains in dorsal striatum of the nonhuman primate are defined by the dynamic behavior of dopamine. J. Neurosci. 22, 5705–5712.

Cragg, S.J., Rice, M.E., 2004. DAncing past the DAT at a DA synapse. Trends Neurosci. 27, 270–277.

Day, J.J., Roitman, M.F., Wightman, R.M., Carelli, R.M., 2007. Associative learning mediates dynamic shifts in dopamine signaling in the nucleus accumbens. Nat. Neurosci. 10, 1020–1028.

Di Paolo, T., Bédard, P., Daigle, M., Boucher, R., 1986. Long-term effects of MPTP on central and peripheral catecholamine and indoleamine concentrations in monkeys. Brain Res. 379, 286–293.

Dommett, E., Coizet, V., Blaha, C.D., Martindale, J., Lefebvre, V., Walton, N., Mayhew, J.E.W., Overton, P.G., Redgrave, P., 2005. How visual stimuli activate dopaminergic neurons at short latency. Science 307, 1476–1479.

Einaga, Y., Sato, R., Olivia, H., Shin, D., Ivandini, T.A., Fujishima, A., 2004. Modified diamond electrodes for electrolysis and electroanalysis applications. Electrochim. Acta 49, 3989–3995.

Fiorillo, C.D., Tobler, P.N., Schultz, W., 2003. Discrete coding of reward probability and uncertainty by dopamine neurons. Science 299, 1898–1902.

Flagel, S.B., Clark, J.J., Robinson, T.E., Mayo, L., Czuj, A., Willuhn, I., Akers, C.A., Clinton, S.M., Phillips, P.E., Akil, H., 2011. A selective role for dopamine in stimulus-reward learning. Nature 469 (7328), 53–57.

Franklin, F., Paxinos, G., 1997. The Mouse Brain in Stereotaxic Coordinates. Academic Press, San Diego.

Fujishima, A., Einaga, Y., Rao, T.N., Tryk, D.A., 2005. Diamond Electrochemistry. Elsevier-BKC.

Garris, P.A., Ciolkowski, E.L., Wightman, R.M., 1994. Heterogeneity of evoked dopamine overflow within the striatal and striatoamygdaloid regions. Neuroscience 59, 417–427.

Garris, P.A., Kilpatrick, M., Bunin, M.A., Michael, D., Walker, Q.D., Wightman, R.M., 1999. Dissociation of dopamine release in the nucleus accumbens from intracranial self-stimulation. Nature 398 (6722), 67–69.

Gerhardt, G.A., Cass, W.A., Hudson, J., Henson, M., Zhang, Z., Ovadia, A., XHoffer, B.J., Gash, D.M., 1996. *In vivo* electrochemical studies of dopamine overflow and clearance in the striatum of normal and MPTP-treated rhesus monkeys. J. Neurochem. 66, 579–588.

Graybiel, A.M., 1995. Building action repertoires: memory and learning functions of the basal ganglia. Curr. Opin. Neurobiol. 5 (6), 733–741.

Hafizi, S., Kruk, Z.L., Stamford, J.A., 1990. Fast cyclic voltammetry: improved sensitivity to dopamine with extended oxidation scan limits. J. Neurosci. Methods 33, 41–49.

Hashemi, P., Dankoski, E.C., Petrovic, J., Keithley, R.B., Wightman, R.M., 2009. Voltammetric detection of 5-hydroxytryptamine release in the rat brain. Anal. Chem. 81, 9462–9471.

Heien, M.L., Phillips, P.E., Stuber, G.D., Seipel, A.T., Wightman, R.M., 2003. Overoxidation of carbon-fiber microelectrodes enhances dopamine adsorption and increases sensitivity. Analyst 128, 1413–1419.

Heien, M.L., Johnson, M.A., Wightman, R.M., 2004. Resolving neurotransmitters detected by fast-scan cyclic voltammetry. Anal. Chem. 76, 5697–5704.

Joshua, M., Adler, A., Mitelman, R., Vaadia, E., Bergman, H., 2008. Midbrain dopaminergic neurons and striatal cholinergic interneurons encode the difference between reward and aversive events at different epochs of probabilistic classical conditioning trials. J. Neurosci. 28, 11673–11684.
Kawagoe, K.T., Zimmerman, J.B., Wightman, R.M., 1993. Principles of voltammetry and microelectrode surface states. J. Neurosci. Methods 48, 225–240.
Kishioka, A., Fukushima, F., Ito, T., Kataoka, H., Mori, H., Ikeda, T., Itohara, S., Sakimura, K., Mishina, M., 2009. A novel form of memory for auditory fear conditioning at a low-intensity unconditioned stimulus. PLoS One 4, e4157.
Kita, J.M., Parker, L.E., Phillips, P.E., Garris, P.A., Wightman, R.M., 2007. Paradoxical modulation of short-term facilitation of dopamine release by dopamine autoreceptors. J. Neurochem. 102, 1115–1124.
Lindsay, W.S., Herndon Jr., J.G., Blakely, R.D., Justice Jr., J.B., Neill, D.B., 1981. Voltammetric recording from neostriatum of behaving rhesus monkey. Brain Res. 220, 391–396.
Marsden, C.A., Joseph, M.H., Kruk, Z.L., Maidment, N.T., O'Neill, R.D., Schenk, J.O., Stamford, J.A., 1988. *In vivo* voltammetry-present electrodes and methods. Neuroscience 25, 389–400.
Matsumoto, M., Hikosaka, O., 2009. Two types of dopamine neuron distinctly convey positive and negative motivational signals. Nature 459, 837–841.
Mitani, N., Einaga, Y., 2009. The simple voltammetric analysis of acids using highly boron-doped diamond macroelectrodes and microelectrodes. J. Electroanal. Chem. 626, 156–160.
Nakazato, T., Akiyama, A., 1999. High-speed voltammetry: dual measurement of dopamine and serotonin. J. Neurosci. Methods 89, 105–110.
Natori, S., Yoshimi, K., Takahashi, T., Kagohashi, M., Oyama, G., Shimo, Y., Hattori, N., Kitazawa, S., 2009. Subsecond reward-related dopamine release in the mouse dorsal striatum. Neurosci. Res. 63, 267–272.
Oyama, G., Yoshimi, K., Natori, S., Chikaoka, Y., Ren, Y.R., Funayama, M., Shimo, Y., Takahashi, R., Nakazato, T., Kitazawa, S., Hattori, N., 2010. Impaired in vivo dopamine release in parkin knockout mice. Brain Res. 1352, 214–222.
Phillips, P.E., Hancock, P.J., Stamford, J.A., 2002. Time window of autoreceptor-mediated inhibition of limbic and striatal dopamine release. Synapse 44, 15–22.
Phillips, P.E., Stuber, G.D., Heien, M.L., Wightman, R.M., Carelli, R.M., 2003. Subsecond dopamine release promotes cocaine seeking. Nature 422, 614–618.
Phillips, P.E., Wightman, R.M., 2003. Critical guidelines for validation of the selectivity of *in vivo* chemical microsensors. Trend Anal. Chem. 22, 509–514.
Pifl, C., Schingnitz, G., Hornykiewicz, O., 1991. Effect of 1-methyl-4-phenyl-1,2,3,6-tetrahydropyridine on the regional distribution of brain monoamines in the rhesus monkey. Neuroscience 44, 591–605.
Rice, M.E., Cragg, S.J., 2004. Nicotine amplifies reward-related dopamine signals in striatum. Nat. Neurosci. 7, 583–584.
Roitman, M.F., Stuber, G.D., Phillips, P.E., Wightman, R.M., Carelli, R.M., 2004. Dopamine operates as a subsecond modulator of food seeking. J. Neurosci. 24, 1265–1271.
Rodríguez, M., Moralesm, I., González-Mora, J.L., Gómez, I., Sabaté, M., Dopico, J.G., Rodríguez-Oroz, M.C., Obeso, J.A., 2007. Different levodopa actions on the extracellular dopamine pools in the rat striatum. Synapse 61, 61–71.
Rollema, H., Alexander, G.M., Grothusen, J.R., Matos, F.F., Castagnoli Jr., N., 1989. Comparison of the effects of intracerebrally administered MPP+ (1-methyl-4-phenylpyridinium) in three species: microdialysis of dopamine and metabolites in mouse, rat and monkey striatum. Neurosci. Lett. 106, 275–281.
Schmitz, Y., Benoit-Marand, M., Gonon, F., Sulzer, D., 2003. Presynaptic regulation of dopaminergic neurotransmission. J. Neurochem. 87, 273–289.
Schultz, W., Apicella, P., Ljungberg, T., 1993. Responses of monkey dopamine neurons to reward and conditioned stimuli during successive steps of learning a delayed response task. J. Neurosci. 13, 900–913.
Schultz, W., Dayan, P., Montague, P.R., 1997. A neural substrate of prediction and reward. Science 275, 1593–1599.
Schultz, W., 2007. Behavioral dopamine signals. Trends Neurosci. 30, 203–210.
Shiotsuki, H., Yoshimi, K., Shimo, Y., Funayama, M., Takamatsu, Y., Ikeda, K., Takahashi, R., Kitazawa, S., Hattori, N., 2010. A rotarod test for evaluation of motor skill learning. J. Neurosci. Methods 189, 180–185.
Shon, Y.M., Lee, K.H., Goerss, S.J., Kim, I.Y., Kimble, C., Van Gompel, J.J., Bennet, K., Blaha, C.D., Chang, S.Y., 2010. High frequency stimulation of the subthalamic nucleus evokes striatal dopamine release in a large animal model of human DBS neurosurgery. Neurosci. Lett. 475, 136–140.
Suzuki, A., Ivandini, T.A., Yoshimi, K., Fujishima, A., Oyama, G., Nakazato, T., Hattori, N., Kitazawa, S., Einaga, Y., 2007. Fabrication, characterization, and application of boron-doped diamond microelectrodes for *in vivo* dopamine detection. Anal. Chem. 79, 8608–8615.
Takikawa, Y., Kawagoe, R., Hikosaka, O., 2004. A possible role of midbrain dopamine neurons in short- and long-term adaptation of saccades to position-reward mapping. J. Neurophysiol. 92, 2520–2529.
Trouillon, R., O'Hare, D., 2010. Comparison of glassy carbon and boron doped diamond electrodes: resistance to biofouling. Electrochimica. Acta 55, 6586–6595.
Venton, B.J., Toyer, K.P., Wightman, M.R., 2002. Response times of carbon fiber microelectrodes to dynamic changes in cathecholamine concentration. Anal. Chem. 74, 539–546.
Voorn, P., Vanderschuren, L.J., Groenewegen, H.J., Robbins, T.W., Pennartz, C.M., 2004. Putting a spin on the dorsal-ventral divide of the striatum. Trends Neurosci. 27, 468–474.
Wanat, M.J., Kuhnen, C.M., Phillips, P.E.M., 2010. Delays conferred by escalating costs modulate dopamine release to rewards but not their predictors. J. Neurosci. 30, 12020–12027.
Wickens, J.R., Budd, C.S., Hyland, B.I., Arbuthnott, G.W., 2007. Striatal contributions to reward and decision making: making sense of regional variations in a reiterated processing matrix. Ann. N. Y. Acad. Sci. 1104, 192–212.
Willis, G.L., Horne, M.K., Donnan, G.A., 1988. Amine accumulation, catecholamine depletion and motor impairment in Macaca fasicularis and the C-57 black mouse after MPTP administration. Prog. Neuropsychopharmacol. Biol. Psychiatry 12, 469–482.
Yavich, L., 1996. Two simultaneously working storage pools of dopamine in mouse caudate and nucleus accumbens. Br. J. Pharmacol. 119, 869–876.
Yavich, L., Tiihonen, J., 2000. Patterns of dopamine overflow in mouse nucleus accumbens during intracranial self-stimulation. Neurosci. Lett. 293, 41–44.
Zachek, M.K., Takmakov, P., Moody, B., Wightman, R.M., McCarty, G.S., 2009. Simultaneous decoupled detection of dopamine and oxygen using pyrolyzed carbon microarrays and fast-scan cyclic voltammetry. Anal. Chem. 81, 6258–6265.
Zhang, T., Zhang, L., Liang, Y., Siapas, A.G., Zhou, F.M., Dani, J.A., 2009. Dopamine signaling differences in the nucleus accumbens and dorsal striatum exploited by nicotine. J. Neurosci. 29, 4035–4043.